

Electron Microscope Study of Sporulation and Parasporal Crystal Formation in *Bacillus thuringiensis*

DONALD B. BECHTEL AND LEE A. BULLA, JR.*

U.S. Grain Marketing Research Center, Agricultural Research Service, U.S. Department of Agriculture, Manhattan, Kansas 66502

Received for publication 11 June 1976

A comprehensive ultrastructural analysis of sporulation and parasporal crystal development is described for *Bacillus thuringiensis*. The insecticidal crystal of *B. thuringiensis* is initiated at the start of engulfment and is nearly complete by the time the exosporium forms. The crystal and a heretofore unobserved ovoid inclusion develop without any clear association with the forespore septum, exosporium, or mesosomes. These observations contradict previous hypotheses that the crystal is synthesized on the forespore membrane, exosporium, or mesosomes. Formation of forespore septa involves densely staining, double-membrane-bound, vesicular mesosomes that have a bridged appearance. Forespore engulfment is subpolar and also involves mesosomes. Upon completion of engulfment the following cytoplasmic changes occur: decrease in electron density of the incipient forespore membrane; loss of bridged appearance of incipient forespore membrane; change in stainability of incipient forespore, forespore, and mother cell cytoplasm; and alteration in staining quality of plasma membrane. These changes are involved in the conversion of the incipient forespore into a forespore and reflect "commitment" to sporulation.

Bacillus thuringiensis is a rod-shaped, aerobic, sporeforming bacterium uniquely characterized by the production, during the sporulation cycle, of one or more proteinaceous parasporal crystals. The organism is distinguished from other bacilli such as *B. cereus* by its pathogenicity for larvae of *Lepidoptera*, which is attributed to the proteinaceous crystal (2). In addition to insecticidal properties, the protein apparently is capable of regressing tumors (26) and enhancing the overall immune response in mammals (27).

Found to be glycoprotein (L. A. Bulla, Jr., K. J. Kramer, D. B. Bechtel, and L. I. Davidson, in D. Schlessinger (ed.), *Microbiology—1976*, in press), the crystal is formed outside the exosporium during stages III to VI of sporulation. Electron microscope studies of the proteinaceous crystal primarily have been concerned with its physical arrangement. The surface was examined using metal-shadowed preparations (11) and carbon replicas (18). X-ray diffractograms provided the crystal unit cell dimensions (15), and thin sections revealed the internal structure (24) from which Norris (23) constructed a hypothetical crystal model. Negatively stained and freeze-etched samples prepared by Norris (23) corroborated the crystal model originally proposed by Holmes and Monro (15).

Although there have been several developmental studies of *B. thuringiensis* reported (1, 29, 32), a comprehensive ultrastructural analysis of the sporulation cycle involving parasporal crystal formation in this organism has not been published. Our study provides an overview of *B. thuringiensis* spore and crystal morphogenesis and describes certain aspects of the sporulation process that are unique to this organism. Particularly, evidence is presented for involvement of vesicular mesosomes in the formation of forespore septa and of forespore membrane. Also, our data contradict the hypotheses that the crystal is synthesized and assembled on forespore membrane (8) or on the exosporium (33, 34).

MATERIALS AND METHODS

Organism and cultural conditions. *B. thuringiensis* strain HD-1 was isolated from Dipel, a commercial insecticide manufactured by Abbott Laboratories, North Chicago, Ill. The strain (HD-1) used in this study has been identified as *B. thuringiensis* subsp. *kurstaki* by H. de Barjac, Institut Pasteur, Paris, France, and is the most toxic for lepidopteran insects. Spore stocks of HD-1 were maintained on modified GYS (21) agar slants at 4°C. Spores, heat-shocked for 30 min at 80°C as previously described (22), were used to inoculate 50 ml of prewarmed (28°C) modified GYS medium contained in a 250-ml Erlenmeyer flask aerated by rotary agitation at 200 rpm. Midexponential cells (10% inoculum) were

transferred three times in the GYS medium maintained at 28°C to obtain synchronously dividing cells. The cells were harvested at midexponential phase by centrifugation at 4°C, and the pellet was suspended in 50 ml of cold GYS medium. The suspension was then equally distributed among five 250-ml Erlenmeyer flasks containing 50 ml of prewarmed (28°C) GYS medium. The cells were incubated in this medium at 28°C with rotary agitation at 200 rpm. Samples (10 ml) of the 50-ml cultures were removed at 30-min intervals, quickly chilled, and centrifuged at 4°C. Sporulation was monitored by phase-contrast and electron microscopy. Greater than 95% of the cells reached stages III and IV synchronously.

Electron microscopy. The pellets were suspended in 4% glutaraldehyde in 0.01 M phosphate-buffered saline at pH 7.2 for 5 min at 4°C. The bacteria were pelleted at 2,000 rpm and suspended in warm (55°C) 2% water agar. The agar was immediately cooled to 4°C, cut into 1-mm cubes, and placed into fresh cold fixative for 1 h. Samples were washed four times in cold buffer for a total of 80 min. After washing, the bacteria were postfixed in buffered 1% OsO₄ at 4°C for 1 h. Samples were washed in double-distilled water for 30 min and stained overnight in 0.5% aqueous uranyl acetate. The bacteria were dehydrated by passing them through a graded acetone series and embedded in either Epon 812 (20) or Spurr resin (35). Samples were cut with a diamond knife

on a Porter-Blum MT-2b ultramicrotome, stained with lead citrate (28), and examined in a Philips EM 201 electron microscope operated at 60 kV. Serial sections, 150 nm thick, were placed on slotted grids previously coated with Formvar and carbon and examined in the microscope at 100 kV.

RESULTS

Overview of sporulation. There are certain sporogenic events, excluding crystal formation, that are unique to *B. thuringiensis* subsp. *kurstaki* although the overall pattern of sporulation in this organism is similar to that of other bacilli (4, 6, 16, 25). The sequence of spore development and parasporal crystal formation in *B. thuringiensis* is diagrammed in Fig. 1 and is summarized here according to the conventional sporulation stages: stage I (7 h), axial filament formation in which there is no apparent involvement of mesosomes with the nucleoid; stage II (7 to 8 h), forespore septum formation involving mesosomes; stage III (8 to 9 h), engulfment with mesosome involvement, first appearance of ovoid inclusion and parasporal crystal, change in stainability of membranes and cytoplasm, and formation of forespore; stages IV to VI (9 to 12 h), formation of exospo-

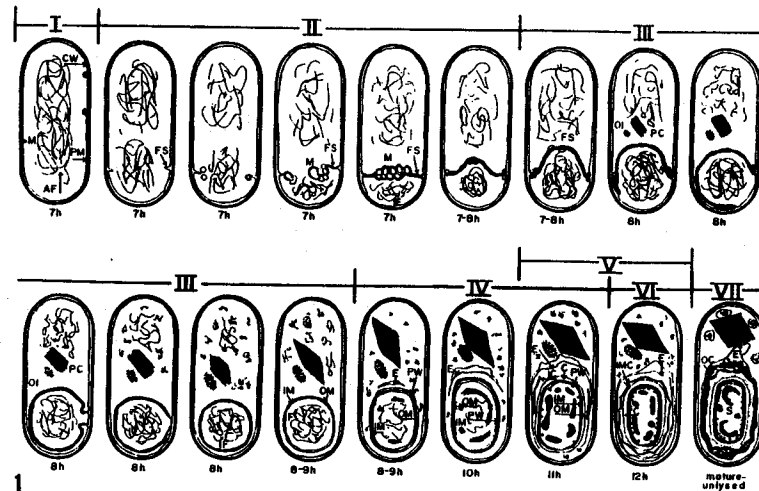


FIG. 1. Diagrammatic scheme of sporulation in *B. thuringiensis*. Abbreviations: M, mesosome; CW, cell wall; PM, plasma membrane; AF, axial filament; FS, forespore septum; IF, incipient forespore; OI, ovoid inclusion; PC, parasporal crystal; F, forespore; IM, inner membrane; OM, outer membrane; PW, primordial cell wall; E, exosporium; LC, lamellar spore coat; OC, outer spore coat; C, cortex; IMC, incorporated mother cell cytoplasm; S, mature spore in an unlysed sporangium.

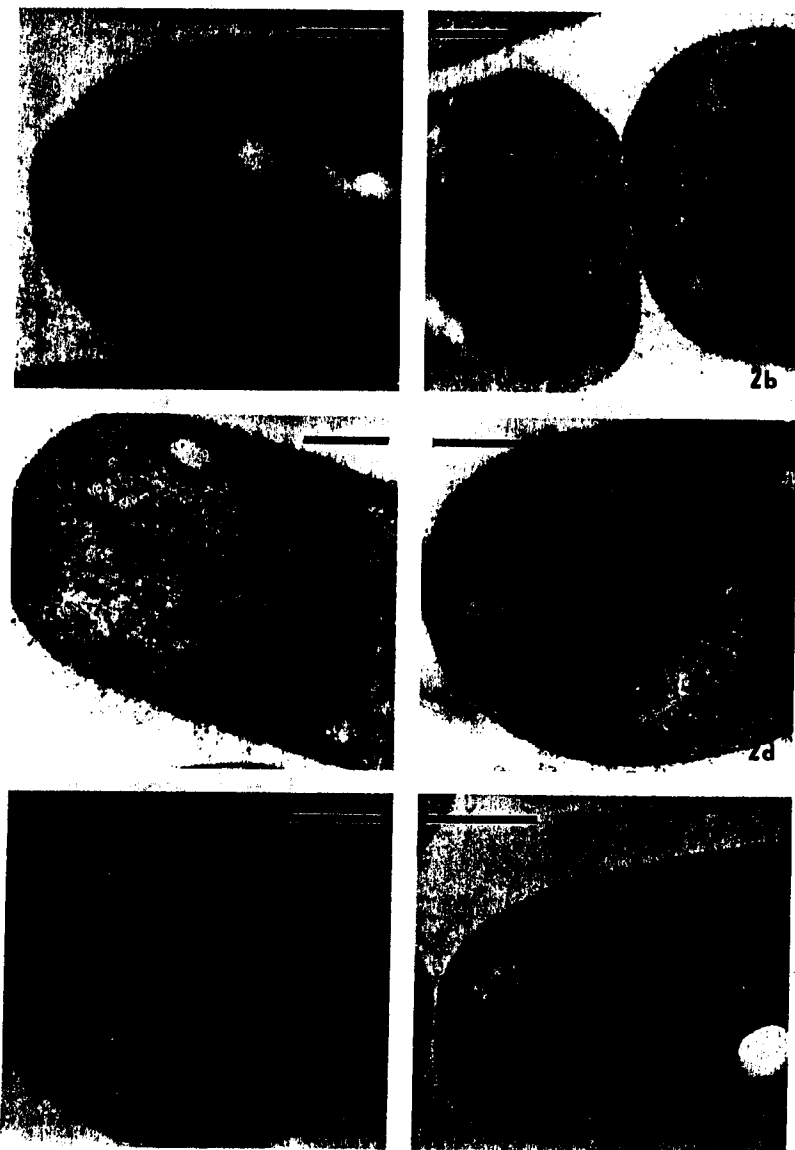


FIG. 2

rium, primordial cell wall, cortex, and spore coats accompanied by transformation of the spore nucleoid; stage VII (post-12 h), spore maturation.

Forespore septum formation—stage II (7 to 8 h). The forespore septa were initiated immediately after stage I and were recognizable as invaginations of the plasma membrane at subpolar regions of the cell (stage II, 7 to 8 h; see arrowhead, Fig. 2a). Mesosomes were associated with the invaginations and were prevalent throughout forespore septum development (Fig. 2a and b). Upon completion of the septum, the area of cytoplasm destined to be incorporated into the forespore was termed the incipient forespore (Fig. 2b and c). The forespore septum was easily distinguished from the vegetative division septum because the former lacked visible cell wall material and was similar in appearance to mesosomal membranes.

Engulfment—stage III (8 to 9 h). Once the forespore septum was complete, engulfment of the incipient forespore commenced. The septum characteristically formed an apex pointed toward the mother cell cytoplasm (see arrow, Fig. 2c). This phenomenon was followed by the movement of the junction of the forespore septum and plasma membrane toward one pole of the cell. The movement was generally greater on one side and resulted in subpolar rather than polar engulfment. Mesosomes were present at the junction of the septum and plasma membrane during engulfment (Fig. 2d). Subpolar engulfment by *B. thuringiensis* is typified in both cross- and longitudinally sectioned cells (Fig. 2e and f).

Completion of engulfment occurred when the septum became detached from the plasma membrane, isolating the incipient forespore from the mother cell cytoplasm. Immediately after septum detachment, several changes occurred which lead to development of the forespore. One of the most noticeable changes was the decrease in electron density of the incipient forespore membrane (Fig. 3a). The incipient

forespore membrane also lost its mesosome-like appearance and was transformed into the inner and outer forespore membranes (compare Fig. 3b and c). A second significant change was in the staining qualities of the mother cell (sporangial) and forespore cytoplasm. The sporangial cytoplasm of cells that had completed engulfment stained more heavily and appeared more granular than either the cytoplasm of forespores or cells not having completed the process (compare cells in Fig. 3a). A third, less conspicuous change occurred in the appearance of the plasma membrane. Prior to engulfment the plasma membrane was irregular and not distinctly trilaminar (see cell A, Fig. 3d). After engulfment, however, the membrane was distinctly trilaminar, with the outer electron-dense portion being thicker than the inner one (see cell B, Fig. 3d).

Spore wall development—stages IV to VI (8 to 13 h). Spore wall development is summarized diagrammatically in Fig. 4 and is detailed in Fig. 3e to i and 5d. The primordial cell wall was the first part of the spore wall to form and was secreted between the inner and outer forespore membranes (stage IV, 8 to 9 h; Fig. 3e and f). Concomitant to primordial cell wall appearance, electron-dense, fibrous masses appeared with the spore nucleoid (Fig. 3e and g); also the mother cell nucleoid began to fragment (Fig. 3g and 5b and c). As the primordial cell wall was secreted, ribosome-like spherical particles became aligned along the lateral sides of the spore where the lamellar spore coat was initiated (arrowheads, Fig. 3h) and remained attached during development of the lamellar coat (stage V, 11 to 13 h; arrowheads, Fig. 3i and 5d). While the lamellar coat was being formed, three other modifications also occurred: (i) the electron-dense, fibrous spore nucleoid (Fig. 3e and g) became an electron-transparent homogeneous structure (Fig. 5d); (ii) the primordial cell wall thickened (Fig. 4); and (iii) the exosporium engulfed the spore (Fig. 5d).

After the primordial cell wall had attained

FIG. 2. Forespore septum development and engulfment in *B. thuringiensis*. (a) Forespore septum development during stage II. Lower septum (FS) has vesicular mesosomes (M) closely associated, whereas upper septum (arrowhead) is still represented as an invagination. $\times 67,500$. Bar = $0.25 \mu\text{m}$. (b) Two newly completed forespore septa (FS) that have isolated the incipient forespore cytoplasm (IF) from the mother cell cytoplasm (MC). Note mesosomes (M) still continuous with septa. $\times 54,000$. Bar = $0.25 \mu\text{m}$. (c) Initiation of engulfment (stage III). Forespore septum extends (arrow) toward mother cell center (MC) forming oval incipient forespore (IF). $\times 61,500$. Bar = $0.25 \mu\text{m}$. (d) Stage III cell showing predominance of mesosomes (M) at one junction of engulfment membrane. Note that engulfment membranes are continuous with plasma membrane at several locations (arrows). IF, Incipient forespore. $\times 61,500$. Bar = $0.25 \mu\text{m}$. (e) Cross section through cell containing incipient forespore (IF) showing connection of engulfment membranes on lateral side of cell (arrowheads). $\times 67,500$. Bar = $0.25 \mu\text{m}$. (f) Longitudinal section through subpolar engulfment (stage III) of incipient forespore (IF). Note subpolar attachment of engulfment membrane to plasma membrane (arrowheads). $\times 38,200$. Bar = $0.5 \mu\text{m}$.

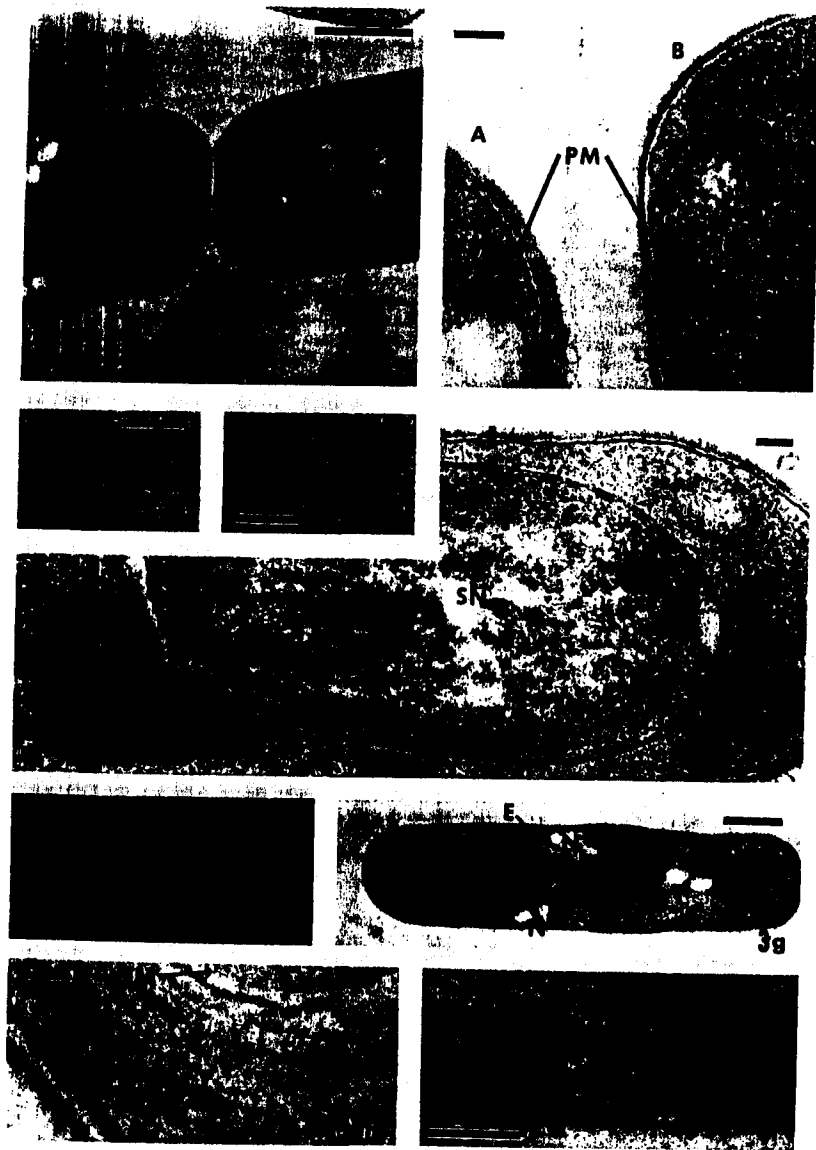


FIG. 3

maximum thickness, the cortex developed (stages IV to VI, 11 to 12 h) between the primordial cell wall and the outer forespore membrane (Fig. 4). After cortex and lamellar spore coat development, the outer fibrous spore coat formed. The mature lysed spore (stage VII) has several distinct layers. Beginning with the inner membrane (see Fig. 4) they are as follows: primordial cell wall, cortex, outer membrane, incorporated mother cell cytoplasm, lamellar spore coat, outer fibrous spore coat, and the exosporium.

Parasporal crystal development—stages III to VI (8 to 12 h). The parasporal crystal of *B. thuringiensis* was observed first during engulfment (stage III, 8 h; Fig. 5a) and possessed crystal lattice fringes at this early stage of development. The crystal was almost full-sized by the time the exosporium appears (stage IV, 9 h; Fig. 1 and 5b and c). An ovoid inclusion developed simultaneously to crystal appearance (Fig. 3e and 5b and c). Some cells lacked this inclusion, however, as evidenced in Fig. 5a. The ovoid inclusion was easily distinguished from the diamond-shaped parasporal crystal in that it lacked crystal lattice fringes and always appeared ovoid. More than one crystal can develop within a cell, but only one ovoid inclusion per sporangium was ever observed. Several different types of crystal lattice shapes were seen; many parasporal crystals lacked lattice fringes. The distance between the parallel lattice fringes is 8.9 nm. Both the parasporal crystal and ovoid inclusion were not consistently associated with a specific structure. Serial sections (not shown) reveal that the crystal was not

connected to mesosomes or to membranes of the incipient forespore, forespore, or exosporium. Although in some micrographs there appears to be an association of the crystal with the forespore membrane, serial sections revealed that the parasporal crystal and forespore were always separated by cytoplasm.

DISCUSSION

One of the most striking aspects of *B. thuringiensis* sporogenesis is the synthesis of the parasporal crystal. Our study reveals that the crystal is initiated during engulfment and is virtually full sized by the completion of this process. The lattice fringes observed during its formation support the view that this body is progressively assembled from subunits to ultimately produce a crystal that refracts light (30). The absence of crystal lattice images in some crystals and the variation of images in others are probably the result of the angle of the crystal axis to the electron beam (17). Kaneko and Matsuhashima (17) demonstrated that by changing the axis of *B. subtilis* crystals in the electron beam, they were able to show various lattice shapes within the same crystal. We observed a similar phenomenon with *B. thuringiensis* crystals (micrographs not shown). The ovoid inclusion observed in this study has not been reported before for *B. thuringiensis*. Its general appearance suggests that it is not of the same composition as the crystal because it does not display crystal lattice fringes and usually stains differently from the crystal. Whether the ovoid inclusion possesses insecticidal properties is not known.

FIG. 3. Forespore and spore wall formation in *B. thuringiensis*. (a) Comparison of cells undergoing engulfment (A) and those that have completed engulfment (B). Note that incipient forespore cytoplasm (IF) and mother cell cytoplasm (MC) of cell A stain differently than the cytoplasm of either the forespore (F) or mother cell of cell B. Also observe the change in stainability of forespore membranes and engulfment membranes. $\times 34,000$. Bar = 0.5 μm . (b) High magnification of engulfment membranes (G). Note dense staining and bridged appearance. IF, Incipient forespore. $\times 235,000$. Bar = 0.05 μm . (c) High magnification of forespore membranes (IM, inner membrane; OM, outer membrane) after engulfment (stage III). Note trilaminar appearance of each membrane. Also, there is a decrease in electron density and a loss of bridged appearance. F, Forespore. $\times 225,000$. Bar = 0.05 μm . (d) High-magnification comparison of cell undergoing engulfment (A) and one that has completed engulfment (B). Note differences between plasma membranes (PM) and staining qualities of cytoplasm. $\times 93,000$. Bar = 0.10 μm . (e) Early stage IV cell showing inner (IM) and outer (OM) membranes with innerspaced primordial cell wall (PW). Observe fibrous regions (Fr) with the spore nucleoid (SN). OI, Ovoid inclusion; E, exosporium. $\times 72,500$. Bar = 0.1 μm . (f) High magnification of spore (S) showing developing primordial cell wall (PW) between inner (IM) and outer (OM) membranes. PM, Plasma membrane; CW, cell wall. $\times 120,000$. Bar = 0.10 μm . (g) Low magnification of sporulating cell (nucleoid (N) completely transformed into fibrous region (Fr) and fragmentation of mother cell nucleoid (N)). Note well-developed parasporal crystal (PC) near newly initiated exosporium (E). $\times 22,500$. Bar = 0.5 μm . (h) High magnification of developing spore (S) showing thickened primordial cell wall (PW) between inner (IM) and outer (OM) membranes. Note ribosome-like particles lined up in region where lamellar spore coat will develop (arrowheads). $\times 215,000$. Bar = 0.05 μm . (i) High magnification of spore (S) as lamellar spore coat (LC) develops. Note ribosome-like particles (arrowheads) on outer surface of lamellar spore coat (LC). Outer membrane (OM) is observed in oblique section. IM, Inner membrane; PW, primordial cell wall; PM, plasma membrane; CW, cell wall. $\times 170,000$. Bar = 0.10 μm .

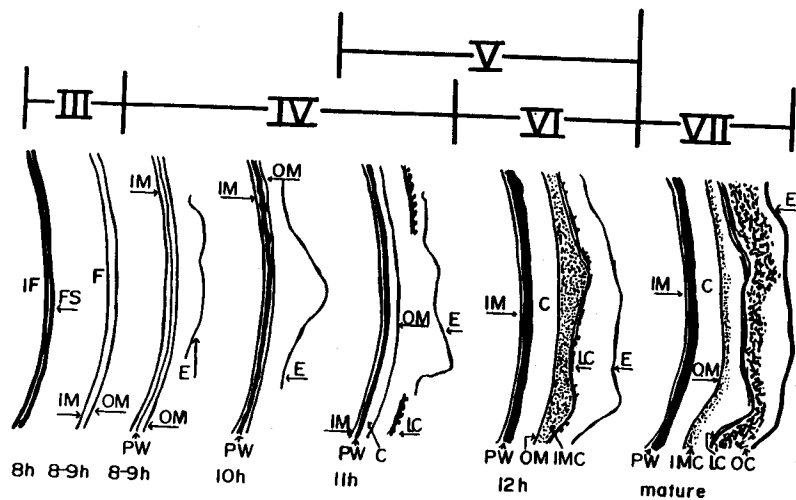


Fig. 4. Diagrammatic scheme of spore wall elaboration in *B. thuringiensis*. Symbols same as for Fig. 1.

The unique subpolar type of engulfment exhibited by *B. thuringiensis* is in contrast to the polar kind described for other sporeforming bacilli (4, 7, 13, 16, 25, 37). Moreover, the large numbers of vesicular mesosomes accompanying the engulfing membrane is unlike the single large mesosome (usually morphological type II or IX according to the categorization of Ghosh [10]) associated with engulfment of some other bacilli (4, 7, 12-14, 16, 25). We also observed the vesicular mesosomes (type VIII after Ghosh) of *B. thuringiensis* in close association with cell division septa (unpublished data) as well as with sporulation septa. They stain densely, are double layered, and are not distinctly trilaminar. Ellar and Lundgren (6) described vesicular areas in *B. cereus* that apparently functioned in forespore septum formation.

Some variation in morphological types of mesosomes has been shown to be greatly affected by fixation procedures (10). Aldehyde fixation (used in this study) tends to reveal mesosomal membranes as being "bridged"; such a structural arrangement usually is not retained with osmium tetroxide fixation (10). For *B. thuringiensis* fixed in aldehyde, the mesosomes, the terminal ends of cell division septa, the forespore septa, and the engulfment membranes all appeared as bridged. Holt et al. (16) fixed *B. sphaericus* in aldehydes and observed lamellar mesosomes without the bridged ap-

pearance. Presumably, the difference in aldehyde fixation qualities between the mesosomes of *B. thuringiensis* and *B. sphaericus* indicates that the mesosomal membranes of these two organisms are different. Whether the mesosomes of *B. thuringiensis* are morphologically distinct from those of the other bacilli reported will probably be resolved by freeze-etching. Because the mesosomes and the septa and engulfment membranes of *B. thuringiensis* all stained similarly and because of the close association of mesosomes and septa, we believe that there is a direct involvement of mesosomes in the synthesis of membrane during cell division and sporulation. However, our studies showed no physical relationship between mesosomes and developing crystals as did Kaneko and Matsushima (17) for *B. subtilis*.

The ultrastructural changes that occurred within the sporulating cell after completion of engulfment could not be related to crystal formation. The dramatic loss of electron density in the incipient forespore membrane probably resulted from its transformation into two distinct trilaminar layers (see Fig. 3a to c). Highton (14) observed a similar reduction in electron density of the forespore membrane of *B. cereus* 569H/24. We have observed that *B. thuringiensis* cells that have reached this particular stage of sporulation are incapable of returning to vegetative growth (unpublished data) and, there-



Fig. 5. Crystal development in *B. thuringiensis*. (a) Sporulating cell (stage III) with parasporal crystal (PC) at opposite end of incipient forespore (IF). $\times 34,800$. Bar = 0.5 μ m. (b) Sporulating cell (stage IV) with parasporal crystal (PC) and forespore (F) at one end and the ovoid inclusion (OI) at the other end. Note exosporium (E) and fragmenting mother cell nucleoid (N). $\times 22,000$. Bar = 0.5 μ m. (c) Sporulating cell (stage IV) with parasporal crystal (PC) at the opposite end of forespore (F) and ovoid inclusion (OI). E, Exosporium; N, fragmenting mother cell nucleoid. $\times 29,000$. Bar = 0.5 μ m. (d) Sporulating cell (stage IV to V) of *B. thuringiensis* showing lamellar spore coat (arrowheads) forming on lateral sides of spore (S). Note that exosporium (E) has nearly enveloped the spore and that the spore nucleoid (SN) has been transformed into an electron-translucent region. Both parasporal crystal (PC) and ovoid inclusion (OI) are near their maximum size. $\times 29,500$. Bar = 0.5 μ m.

fore, we conclude that the decrease in electron density of the forespore membrane reflects "commitment" to sporulation. Whether the increased electron density and granulation of the mother cell (sporangial) cytoplasm is characteristic of senescence or reflects a change in plasma membrane permeability or both is not known. The increase in density of the outer portion of the plasma membrane upon completion of engulfment has been interpreted as a

change in the molecular structure of the membrane, which consequently alters its permeability (14). Freeze et al. (9) demonstrated diminution of the membrane-associated glucose-phosphoenolpyruvate transferase system after vegetative growth of *B. subtilis*. Lang and Lundgren (19) showed quantitative changes in membrane lipid composition during sporulation of *B. cereus*. Also, Bulla et al. (3) observed depression of membrane-bound enzyme activi-

ties of *B. thuringiensis* involved with energy production by the electron transport system and oxidation of acetyl coenzyme A via terminal respiratory pathways, i.e., tricarboxylic acid and glyoxylic acid cycles. Another implication of the change in electron density of the plasma membrane is the active transport of cations (5, 31). Scribner et al. (31) described active transport of potassium, magnesium, calcium, and manganese and demonstrated that each cation transport system is independently regulated during sporulation, resulting in various rates of cation uptake. Coincidentally, calcium and potassium uptake was high during forespore formation (31, 36).

The results of our observations indicate that there is no involvement of the exosporium with crystal formation and is in contrast to the postulation that the parasporal crystal of *B. thuringiensis* is synthesized on this structure (33, 34). Our present study and that of Young and Fitz-James (38) reveal that the crystal is formed during engulfment and is almost complete by the end of this process. Furthermore, the exosporium forms at least 1 h after completion of engulfment (see Fig. 1). These observations indicate no involvement of the exosporium with crystal formation. The fact that the crystal can develop with no apparent association of the forespore membrane dispels the notion that it is synthesized on this membrane (8). That the crystal is not synthesized on the forespore membrane was substantiated by serial sections and numerous high-magnification micrographs (not shown). We surmise that the parasporal crystal of *B. thuringiensis* is formed within the cytoplasm without any apparent involvement of mesosomes, forespore septa, forespore membrane, or exosporium.

LITERATURE CITED

- Aronson, J. N., P. A. Bowe, and J. Swafford. 1967. Mesosomes in *m*-tyrosine-inhibited *Bacillus thuringiensis*. *J. Bacteriol.* 93:1174-1176.
- Buchanan, R. E., and N. E. Gibbons. 1974. *Bergey's manual of determinative bacteriology*, p. 536. The Williams & Wilkins Co., Baltimore, Md.
- Bulla, L. A., Jr., G. St. Julian, and R. A. Rhodes. 1971. Physiology of sporeforming bacteria associated with insects. III. Radiospirometry of pyruvate, acetate, succinate, and glutamate oxidation. *Can. J. Microbiol.* 17:1073-1079.
- Decker, B., and S. Maier. 1975. Fine structure of mesosomal involvement during *Bacillus macerans* sporulation. *J. Bacteriol.* 121:363-372.
- Eisenstadt, E., and S. Silver. 1972. Calcium transport during sporulation in *Bacillus subtilis*, p. 180-186. In H. D. Halvorson, R. Hanson, and L. L. Campbell (ed.), *Spores V*. American Society for Microbiology, Washington, D.C.
- Ellis, D. J., and D. G. Lundgren. 1966. Fine structure of sporulation in *Bacillus cereus* grown in a chemically defined medium. *J. Bacteriol.* 92:1748-1764.
- Fitz-James, P. C. 1960. Participation of the cytoplasmic membrane in growth and spore formation of bacilli. *J. Biophys. Biochem. Cytol.* 8:507-528.
- Fitz-James, P. C. 1962. The initial formation of parasporal inclusions in bacilli, p. RR-10. In Sidney S. Broese, Jr. (ed.), *Fifth International Congress for Electron Microscopy*, Philadelphia, August 29-September 5, 1962. Academic Press Inc., New York.
- Freeze, E., W. Klofat, and E. Gallus. 1970. Commitment to sporulation and induction of glucose-phosphoenolpyruvate transferase. *Biochim. Biophys. Acta* 222:265-289.
- Ghoosh, B. K. 1974. The mesosome—a clue to the evolution of the plasma membrane. *Sub-Cell. Biochem.* 3:311-367.
- Hannay, C. L., and P. C. Fitz-James. 1956. The protein crystals of *Bacillus thuringiensis* Berliner. *Can. J. Microbiol.* 1:694-710.
- Highton, P. J. 1969. An electron microscopic study of cell growth and mesosome structure of *Bacillus licheniformis*. *J. Ultrastruct. Res.* 26:130-147.
- Highton, P. J. 1970. An electron microscopic study of the structure of mesosomal membranes in *Bacillus licheniformis*. *J. Ultrastruct. Res.* 31:247-259.
- Highton, P. J. 1972. Changes in the structure and mesosomes and cell membrane of *Bacillus cereus* during sporulation, p. 13-18. In H. O. Halvorson, R. Hanson, and L. L. Campbell (ed.), *Spores V*. American Society for Microbiology, Washington, D.C.
- Holmes, K. C., and R. E. Monro. 1965. Studies on the structure of parasporal inclusions of *Bacillus thuringiensis*. *J. Mol. Biol.* 14:572-581.
- Holt, S. C., J. J. Gauthier, and D. J. Tipper. 1975. Ultrastructural studies of sporulation in *Bacillus sphaericus*. *J. Bacteriol.* 122:1322-1338.
- Kaneko, I., and H. Matsushima. 1975. Crystalline inclusions in sporulating *Bacillus subtilis* cells, p. 580-585. In P. Gerhardt, R. N. Costilow, and H. L. Sadoff, (ed.), *Spores VI*. American Society for Microbiology, Washington, D.C.
- Labaw, L. W. 1964. The structure of *Bacillus thuringiensis* Berliner crystals. *J. Ultrastruct. Res.* 10:66-75.
- Lang, D. R., and D. G. Lundgren. 1970. Lipid composition of *Bacillus cereus* during growth and sporulation. *J. Bacteriol.* 101:483-489.
- Luft, J. 1961. Improvements in epoxy resin embedding methods. *J. Biophys. Biochem. Cytol.* 9:409-414.
- Nickerson, K. W., and L. A. Bulla, Jr. 1974. Physiology of sporeforming bacteria associated with insects: minimal nutritional requirements for growth, sporulation, and parasporal crystal formation in *Bacillus thuringiensis*. *Appl. Microbiol.* 28:124-128.
- Nickerson, K. W., and L. A. Bulla, Jr. 1975. Lipid metabolism during bacterial growth, sporulation, and germination: an obligate nutritional requirement in *Bacillus thuringiensis* for compounds that stimulate fatty acid synthesis. *J. Bacteriol.* 123:598-603.
- Norris, J. R. 1971. The protein crystal toxin of *Bacillus thuringiensis* biosynthesis and physical structure, p. 229-246. In H. D. Burges and N. W. Hussey (ed.), *Microbial control of insects and mites*. Academic Press Inc., London.
- Norris, J. R., and D. H. Watson. 1960. An electron microscope study of sporulation and protein crystal formation in *Bacillus cereus* var. *alesti*. *J. Gen. Microbiol.* 22:744-749.
- Obye, D. F., and W. G. Murrell. 1962. Formation and structure of the spore of *Bacillus coagulans*. *J. Cell Biol.* 14:111-123.
- Prasad, S. S. S. V., and Y. I. Shethna. 1974. Purification, crystallization and partial characterization of the antitumour and insecticidal protein subunit from the δ -endotoxin of *Bacillus thuringiensis* var. *thuringiensis*. *Biochim. Biophys. Acta* 363:558-566.
- Prasad, S. S. S. V., and Y. I. Shethna. 1975. Enhancement of immune response by the proteinaceous crystal of *Bacillus thuringiensis* var. *thuringiensis*. *Biochem. Biophys. Res. Commun.* 62:517-523.
- Reynolds, E. S. 1963. The use of lead citrate at high pH as an electron-opaque stain in electron microscopy. *J. Cell Biol.* 17:208-212.
- Ribier, J., and M. M. Lecadet. 1974. *Bacillus thuringiensis* var. *Berliner* 1715: sporulation of a mutant cristal-participation des mesosomes a la formation des enveloppes sporales (exosporium et tunique). *C.R. Acad. Sci. Ser. D* 278:1131-1134.
- Rogoff, M. H., and A. A. Yousten. 1969. *Bacillus thuringiensis*: microbial considerations. *Annu. Rev. Microbiol.* 23:357-386.
- Scribner, H. E., J. Mogelson, E. Eisenstadt, and S. Silver. 1975. Regulation of cation transport during bacterial sporulation, p. 346-355. In P. Gerhardt, R. N. Costilow, and H. L. Sadoff (ed.), *Spores VI*. American Society for Microbiology, Washington, D.C.
- Short, J. A., P. D. Walker, R. O. Thomson, and H. J. Somerville. 1974. The fine structure of *Bacillus finitimus* and *Bacillus thuringiensis* spores with special reference to the location of crystal antigen. *J. Gen. Microbiol.* 84:261-276.
- Somerville, H. J. 1971. Formation of the parasporal inclusion of *Bacillus thuringiensis*. *Eur. J. Biochem.* 18:226-237.
- Somerville, H. J., and C. R. James. 1970. Association of the crystalline inclusion of *Bacillus thuringiensis* with the exosporium. *J. Bacteriol.* 102:580-583.
- Spurr, A. R. 1969. A low-viscosity epoxy resin embedding medium for electron microscopy. *J. Ultrastruct. Res.* 26:31-43.
- Vinter, V. 1969. Physiology and biochemistry of sporulation, p. 73-123. In G. W. Gould and A. Hurst (ed.), *The bacterial spore*. Academic Press Inc., London.
- Walker, P. D. 1970. Cytology of spore formation and germination. *J. Appl. Bacteriol.* 33:1-12.
- Young, I. E., and P. C. Fitz-James. 1959. Chemical and morphological studies of bacterial spore formation. II. Spore and parasporal protein formation in *Bacillus cereus* var. *alesti*. *J. Biophys. Biochem. Cytol.* 6:483-498.